

# Mechanical Advantage of a Hypotrochoid Mechanism

Branimir Vidinsky, MSME  
Vidinsky Engineering

## Abstract

---

This paper presents a new kind of hypotrochoid mechanism with exceptional features. It is a rotational planetary mechanism with harmonic motion. The change of the gear ratio creates a family of mechanisms with a different frequency of this harmonic motion. Another feature of the hypotrochoid mechanism is the closed kinematic chain as a kinematic equivalent. A modified Gruebler criterion for this new kinematic structure is proposed. The mechanical advantage, which is the subject of this study, is the most important feature of the hypotrochoid mechanism. The mechanical advantage of the first two family members is approximately 2.3 to 3 times higher than the inline slider crank mechanism.

---

20<sup>th</sup> December 2021

---

Keywords: mechanical advantage, hypotrochoid, planetary, Gruebler, slider-crank

“Give Me a Place to Stand on, and I Will Move the Earth.”  
Archimedes of Syracuse (c. 287 – c. 212 BC)

## 0. Introduction

A new kind of trochoid mechanisms has recently been synthesized as a result of an effort to create a valveless rotary machine. Literature search [6] to [12] did not establish the existence of such a mechanism. These trochoid mechanisms are planar planetary gear mechanisms with one degree of freedom, the motion of the planetary gears being epicyclic or hypocyclic. The type of planetary transmission and number of gears split these mechanisms into 4 families. Each family has similar kinematic diagrams, Gruebler criterion and loop equations. The hypotrochoid mechanism (HM) introduced in this paper represents such a family of mechanisms.

Chapter 1 describes in detail the HM kinematic diagrams with the appropriate notations used in this paper. Chapter 2 presents the kinematic equivalent diagram with the appropriate generalized notations used for the loop equations, and gives the loop equations necessary for this paper. The HM "index of merit" is in Chapter 3. Here the motivation for the HM mechanical advantage criterion is present, as well the criterion itself with the research method for this paper. Chapter 3 sets the limits of this study, i.e. the HM prototypical parameters number and their range. Chapter 3 also contains the graphical simplification and presentations used in this paper. Chapter 4 is a substantial part of the research. The goal here is to create relations between the input and output forces using the kinematic parameters defined in Chapter 2. Chapter 5 illustrates HM mechanical advantage graphics and their maximum values for the fixed HM parameters in Chapter 3. Chapter 6 is about the validation software, the criterion for validation parameters, and the validation data with illustrations. The equations for slider crank mechanism mechanical advantage, using the criterion and method defined in Chapter 3 are in Chapter 7. Chapter 7 also presents the maximum values of slider crank mechanism mechanical advantage for parameters equivalent to the HM parameters used in Chapter 5. Chapter 8 is a critical discussion about the achievements of this study. Chapter 9 presents the author's opinion about the results of this research.

## 1. Description

### 1.1 History

In 1725, Daniel Bernoulli (1700-1782) discovered a fundamental property of the hypocycloid [1],[2]. He showed that the same hypocycloid can be generated by two different moving circles. This discovery is known as the Complement Theorem. Fig. 1 is an illustration of this hypocycloid feature.

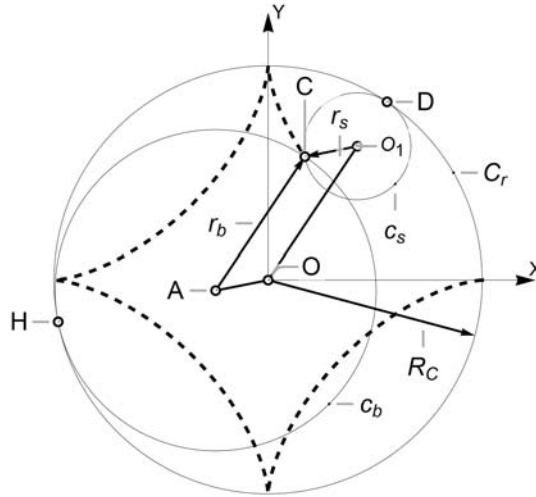


Fig. 1 - Complement generation of a hypocycloid (astroid)

Legend: OA - ex centric distance of big generation circle  $c_b$ ;  $OO_1$  - ex centric distance of small generation circle  $c_s$ ; AC - radius  $r_b$  of big generation circle  $c_b$ ;  $O_1C$  - radius  $r_s$  of small generation circle  $c_s$ ;  $R_C$  - radius of large outside (ring) circle  $C_r$ ;

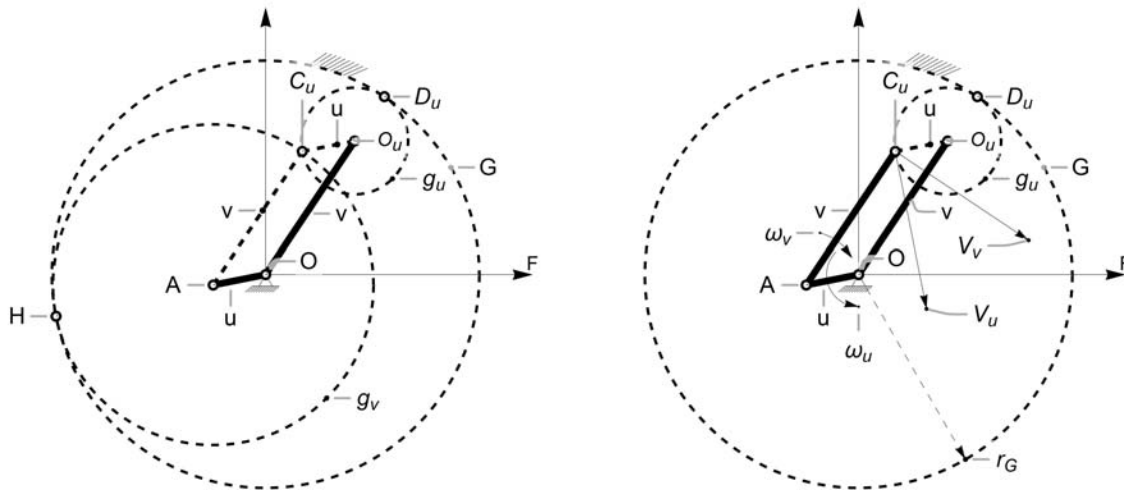
The condition for complement generation is

$$r_b + r_s = R_C \tag{1}$$

where:  $r_b$  - radius of big generation circle  $c_b$ ;  $r_s$  - radius of small generation circle  $c_s$ ;  $R_C$  - radius of large outside (ring) circle  $C_r$ ;  $r_b, r_s$  and  $R_C$  must be natural (positive integer) numbers;

### 1.2 Synthesis

Fig. 2a is a kinematic diagram of an analog mechanism of the complement generation of a hypocycloid, which was an important step toward the creation of a fundamental kinematic chain for the new mechanism. Fig. 2b presents a kinematic diagram of this chain.



a) Complement theorem

b) Parallelogram crank chain

Fig. 2 - Kinematic diagrams of a parallelogram crank chain synthesis

Legend for Fig. 2a: OA - carrier  $u$  for big planetary gear  $g_v$ ;  $OO_u$  - carrier  $v$  for small planetary gear  $g_u$ ;  $AC_u$  - radius  $v$  of big planetary gear  $g_v$ ;  $C_u O_u$  - radius  $u$  of small planetary gear  $g_u$ ;  $G$  - internal (ring) gear;

Legend for Fig. 2b: OA - crankshaft  $u$  of parallelogram crank chain  $OAC_u O_u$ ;  $OO_u$  - carrier  $v$  for planetary gear  $g_u$ ;  $AC_u$  - link  $v$  connecting crankshaft  $u$  with radius  $u$  of planetary gear  $g_u$ ;  $C_u O_u$  - radius  $u$  of planetary gear  $g_u$ ;  $r_G$  - radius of internal (ring) gear  $G$ ;

The kinematic equivalent of the complement theorem modifies Bernoulli complement generation condition (1)

$$u + v = r_G \quad (2)$$

where :  $r_G$  – radius of internal gear  $G$ ;  $u$  – radius of planetary gear  $g_u$ ;  $v$  – length of planetary gear carrier;

The hypocycloid gear ratio is

$$R = \frac{G_r}{g_{ru}} = \frac{r_G}{u} \quad (3)$$

where :  $R$  – gear ratio;  $G_r$ ,  $r_G$  – radius of internal gear  $G$ ;  $g_{ru}$ ,  $u$  – radius of planetary gear  $g_u$ ;

There is another restriction for the presented family of mechanisms on hypocycloid gear ratio  $R$ : gear ratio  $R$  must be a positive integer equal to 3 or higher.

Parallelogram crank chain (PCC)  $OAC_u O_u$  is a planar constant velocity (CV) chain which transmits velocity and power from one pair of links to another. Fig.2b illustrates the equal velocities at point  $C_u$  generated by planetary gear radius  $u$  and PCC link  $v$ . Providing that equal velocities act on links with different length and different rotation direction, the angular velocities of those links are inversely proportional to their lengths with inverse rotation direction. PCC  $OA_u C_u O_u$  exposes an implicit hypocycloid feature that its geometric and kinematic properties have a simple relationship:

$$m = \frac{OO_u}{O_u C_u} = \frac{AC_u}{OA} = \frac{v}{u} = \left| \frac{\omega_u}{-\omega_v} \right| \quad (4)$$

where :  $OO_u$ ,  $v$  – carrier  $v$  for small planetary gear  $g_u$ ;  $O_u C_u$ ,

$u$  – radius of planetary gear  $g_u$ ;  $\omega_u$  – angular velocity of planetary gear  $g_u$ ;

$\omega_v$  – angular velocity of planetary carrier  $v$ ;  $m$  – HM prototypical parameter (angular modulus)

Assuming

$$g_{ru} = u = O_u C_u = OA = -\omega_v = 1 \quad (5)$$

from equations (2), (3) and (4) is obtained

$$R = m + 1 \quad (6)$$

where :  $R$  - gear ratio;  $m$  - HM prototypical parameter (angular modulus)

!!!Important note: The assumption in (5) creates the hypocycloid geometrical structure of PCC  $OAC_u O_u$  and equates the kinematic relations to the geometry - assuming  $-\omega_v = 1$  makes  $\omega_u = -m$  according to (4). Angular modulus  $m$  is the speed ratio of PCC  $OAC_u O_u$ .

PCC  $OAC_u O_u$  transmits the power of the planetary gear  $g_u$  ( $O_u C_u$ ) to crank  $u$  ( $OA_u$ ) through links  $v$  ( $A_u C_u$  and  $OO_u$ ) and vice versa.

HM prototypical parameter (angular modulus)  $m$  controls the relationship between crankshaft and carrier and their angular velocities

### 1.3 Invariants

HM prototypical parameter (angular modulus)  $m$  controls the PCC  $OA_u C_u O_u$  angular position as described.

From (4) link  $OA$  has an  $m$  times higher angular velocity than link  $OO_u$ . If link  $OA$  (Fig. 3) rotates  $2\pi$  radians counterclockwise, link  $OO_u$  will rotate  $2\pi / m$  radians clockwise, and this new position of link  $OO_u$  will be indistinguishable for (invariant to) link  $OA$ . When link  $OA$  rotates  $2m\pi$  radians, link  $OO_u$  will coincide with its initial position. Thus the rotation of link  $OA$  creates  $(m - 1)$  invariant links during its cycle. Fig. 3 a and b shows all invariants of parallelogram crank chain  $OA_u C_u O_u$  after  $2(m - 1)\pi$  rotations of link  $OA$  for angular modulus 2 and 3. (A brief explanation of the rotational invariants according to [3] is in Appendix A)



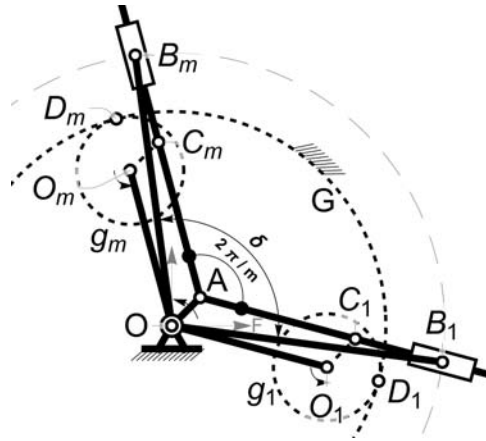


Fig. 5 - HM first and last link kinematic diagram. (for clarity the other links are omitted)

Legend: OA - crankshaft;  $OO_1$  - first planetary carrier rod;  $OAC_1O_1$  - first parallelogram crank chain;  $O_1D_1$  - first planetary gear radius;  $AB_1$  - first variable link (rod of rotor);  $OB_1$  - first invariable link (piston link);  $OO_m$  - last planetary carrier rod;  $OAC_mO_m$  - last parallelogram crank chain;  $O_mD_m$  - last planetary gear radius;  $AB_m$  - last variable link (rod of rotor);  $OB_m$  - last invariable link (piston link); G - internal gear;  $g_1$  - first planetary gear;  $g_m$  - last planetary gear; F - frame of reference;  $2\pi/m$  - invariable angle between the variable links AB;  $\delta$  - variable angle between invariable links OB;

## 2. Kinematic Equivalent

The total control of HM prototypical parameter  $m$  over PCC  $OAC_mO_m$  allows creating an HM abstraction i.e. the HM kinematic equivalent in Fig. 6.

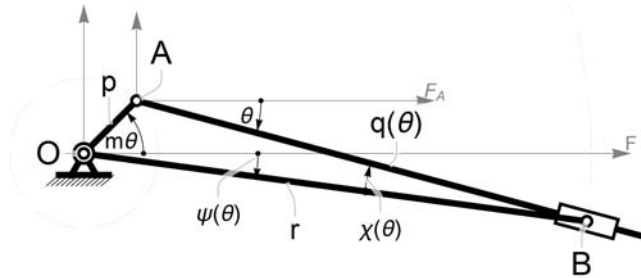


Fig. 6 - HM kinematic equivalent diagram

Legend:  $p = OA$  - crankshaft;  $r = OB$  - invariable link (piston link);  $q(\theta) = AB$  - variable link (rod of rotor);  $\psi(\theta)$  - variable angle between the frame and invariable link OB (pressure angle);  $\chi(\theta)$  - variable angle between invariable link OB and variable link AB (transmission angle);  $m, \theta$  - HM prototypical parameters;

Note: In this study, the notation of functions  $\psi(\theta)$ ,  $\chi(\theta)$  and  $q(\theta)$  indicates functional dependance of angle  $\theta$ . Whenever necessary the sign of rotation direction will be shown explicitly. The parameters values of  $m, \theta, p$ , and  $r$  will be indicated in the figures. Parameters  $m, p$ , and  $r$ , will not be present in the description of equations.

The HM kinematic equivalent is not a mechanism because it does not have a stationary link [4], [6], [7]. It is a closed kinematic chain (CKC) with two stationary joints - one dependent and one independent - in one place. It is an inverted slider-crank without the stationary pivot and with one dependent joint at the other pivot. The description of this CKC is rRPRR, where the lower case "r" stands for the dependent joint. The dependent joint has all three degrees of freedom removed. For this reason, CKC still has 1 DOF. In this case, the Gruebler criterion[5], [6], [7] will take a new form

$$F_{\text{chain}} = 3(n - 1) - 2(j - 1) \quad (7)$$

where  $F_{\text{chain}}$  - DOF;  $n$  - number of links;  $j$  - number of all joints.

### 2.1 Considerations Regarding the HM Kinematic Equivalent

The classical constraint of 4R linkage [7], [8], which gives the relationship between input and output angles, is not applicable in this case. The reasons are two. Firstly, the constant radius link is an output link with a circular path. The square of this link eliminates the angular

output variable, which is unknown, and the system does not have a solution. Secondly and most importantly, the output angular variable is by design a function of the input angular variable.

## 2.2 Position Loop Equations

The HM kinematic equivalent is used for loop equations derivation. The constraint equation is given by the variable distance between the two rotating pivots  $A$  and  $B$ . For notations see Fig. 6.

$$C : A + (B - A) = B$$

$$\text{where : } A = p \begin{bmatrix} \cos(m\theta) \\ \sin(m\theta) \end{bmatrix}; (B - A) = q(\theta) \begin{bmatrix} \cos(-\theta) \\ \sin(-\theta) \end{bmatrix} = q(\theta) \begin{bmatrix} \cos(\theta) \\ -\sin(\theta) \end{bmatrix}; B = r \begin{bmatrix} \cos(\psi(\theta)) \\ \sin(\psi(\theta)) \end{bmatrix} = r \begin{bmatrix} \cos(\psi(\theta)) \\ -\sin(\psi(\theta)) \end{bmatrix}; \quad (8)$$

Note: argument  $(\theta)$  is a positive number, but it has a negative rotation direction by definition in (8).  $(\theta + \alpha)$  creates a rotation  $(-\theta - \alpha)$ ;  
 Function  $(m\theta)$  is a positive number, and it has a positive rotation direction by definition in (8).

Proper substitution yields a system similar to [7], [8]:

$$S(\theta) \cos(\psi(\theta)) + T(\theta) \sin(\psi(\theta)) = U(\theta, m)$$

$$\text{where : } S(\theta) = r \sec(\theta); T(\theta) = -r \csc(\theta); U(\theta) = p (\sec(\theta) \cos(m\theta) + \csc(\theta) \sin(m\theta)); \quad (9)$$

The hypotrochoid geometry requires different angular substitution than accepted for most mechanisms [8]:

$$\sin \mu = \frac{S(\theta)}{\sqrt{S(\theta)^2 + T(\theta)^2}}, \quad \cos \mu = \frac{T(\theta)}{\sqrt{S(\theta)^2 + T(\theta)^2}}, \quad \mu = \tan^{-1}\left(\frac{S(\theta)}{T(\theta)}\right) \quad (10)$$

to obtain the final result for the variable angle

$$\psi(\theta) = \theta - \sin^{-1}\left(\frac{p \sin(\theta(m+1))}{r}\right) \quad (11)$$

It is easy to prove that the transmission angle is

$$\chi(\theta) = \sin^{-1}\left(\frac{p \sin(\theta(m+1))}{r}\right) \quad (12)$$

Now the variable link  $(B - A)$  is

$$q(\theta) = \sqrt{\left(p^2 + r^2 - 2pr \cos\left(\theta(m+1) - \sin^{-1}\left(\frac{p \sin(\theta(m+1))}{r}\right)\right)\right)} \quad (13)$$

### 2.2.1 Links Position Illustrations

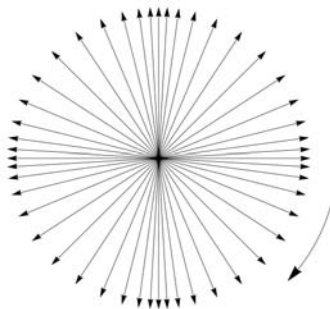


Fig. 7 - Positions of link OB  
 $m = 3; \theta\text{-range} = 0 - 2\pi$

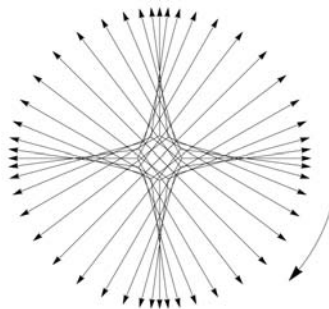


Fig. 8 - Positions of link AB  
 $m = 3; \theta\text{-range} = 0 - 2\pi$

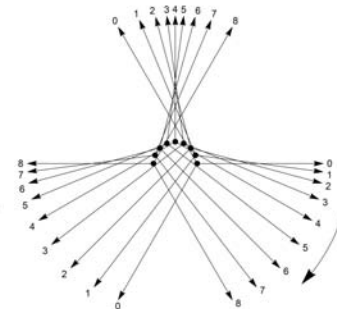


Fig. 9 - Positions of rotor BAB  
 $m = 3; \theta\text{-range} = 0 - \pi/3$

Fig. 7 illustrates (11), which determines the link OB position. One can observe how the point accelerates and decelerates symmetrically. The same (11) determines in Fig. 8 links AB.

The power of HM is in its multirod rotor BAB with a constant angular difference  $2\pi/m$  between links AB. Fig. 9 illustrates rotor BAB motion. It is clear from this figure that while the first rod accelerates, the second one decelerates, and the third rod is in an intermediate position.

## 2.3 Velocity Loop Equations of the HM Kinematic Equivalent

$$\dot{C} : \frac{d}{dt} \mathbf{A} + \frac{d}{dt} (\mathbf{B} - \mathbf{A}) = \frac{d}{dt} \mathbf{B}$$

where :

$$\frac{d}{dt} \mathbf{A} = p \begin{bmatrix} -\sin(m\theta) \\ \cos(m\theta) \end{bmatrix} m \dot{\theta}$$

$$\frac{d}{dt} \mathbf{B} = r \left( 1 - \frac{(m+1)p \cos((m+1)\theta)}{\sqrt{r^2 - p^2 \sin^2((m+1)\theta)}} \right) \begin{bmatrix} -\sin\left(\theta - \sin^{-1}\left(\frac{p \sin((m+1)\theta)}{r}\right)\right) \\ -\cos\left(\theta - \sin^{-1}\left(\frac{p \sin((m+1)\theta)}{r}\right)\right) \end{bmatrix} \dot{\theta}$$

$$\frac{d}{dt} (\mathbf{B} - \mathbf{A}) = \begin{pmatrix} -r \left( 1 - \frac{(m+1)p \cos((m+1)\theta)}{\sqrt{r^2 - p^2 \sin^2((m+1)\theta)}} \right) \sin\left(\theta - \sin^{-1}\left(\frac{p \sin((m+1)\theta)}{r}\right)\right) + p \sin(m\theta) m \\ -r \left( 1 - \frac{(m+1)p \cos((m+1)\theta)}{\sqrt{r^2 - p^2 \sin^2((m+1)\theta)}} \right) \cos\left(\theta - \sin^{-1}\left(\frac{p \sin((m+1)\theta)}{r}\right)\right) - p \cos(m\theta) m \end{pmatrix} \dot{\theta}$$

### 3. “Index of Merit”

#### 3.1 Preliminary

The world of mechanisms is immense. Each and every one of them has specific parameters “that tell whether a mechanism is acceptable for a particular application. Many such parameters have been defined by various authors over the years, and there is no common agreement on a single ‘index of merit’ for all mechanisms.”[9].

#### 3.2 Criterion for Mechanical Advantage

Another fundamental feature of HM is the steady change of the angle between two adjacent links OB (piston links) following the steady rotation of rotor BAB and crankshaft OA. The angle between link OB and the frame is  $\psi(\theta)$  - see Fig. 6. The angle between two adjacent links of rotor BAB is  $2\pi/m$  according to Fig. 5. The angle, in clockwise direction, between two adjacent links of rotor BAB determines the angle between two corresponding links OB. The angle, in clockwise direction, between the first pair of links OB is:

$$\delta(\theta, m) = \psi\left(\theta + \frac{2\pi}{m}, m\right) - \psi(\theta, m) \quad (15)$$

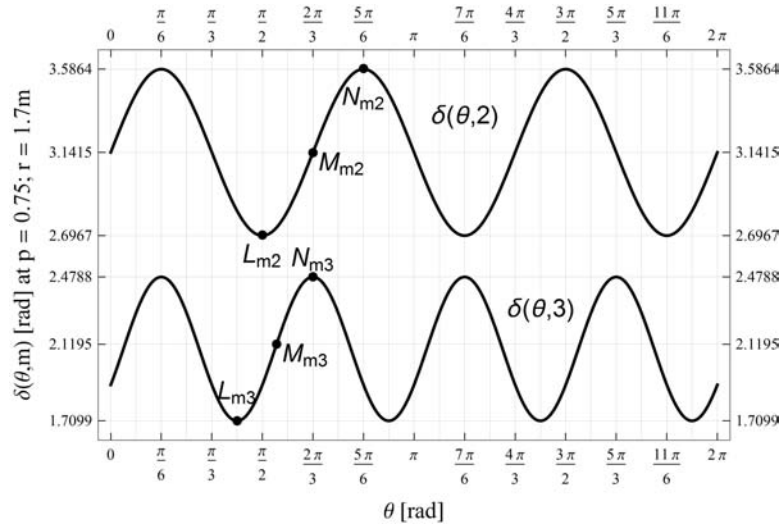


Fig. 10 - Angular difference between the first pair of adjacent links OB -  $\delta(\theta, m)$

Legend: states  $L_m$  - minimum  $\theta$  - value; states  $M_m$  - middle  $\theta$  - value; states  $N_m$  - maximum  $\theta$  - value;

Fig. 10 shows the angular change  $\delta(\theta, m)$  between the first two adjacent links OB, in clockwise direction, for angular modulus  $m = 2$ ,  $m = 3$ , with parameters  $p = 3/4$ ,  $r = 1.7m$ . Parameters  $p = 3/4$ ,  $r = 1.7m$  are not explicitly shown in (15), regardless of the fact that they exist in function  $\psi(\theta)$  and determine the amplitude of  $\delta(\theta)$ . The purpose of this omission is to emphasize the role of the angular modulus in function  $\delta(\theta)$ . Angular modulus  $m$  determines the frequency of function  $\delta(\theta)$ .

The angular change  $\delta(\theta, m)$  in Fig. 10 is a harmonic motion between two adjacent links OB, inducing rotor BAB and crankshaft OA harmonic motion.

Assuming that a pressure input force creates the motion, measuring the output force will define the mechanical advantage of the mechanism.

For this reason, the mechanical advantage criterion, in this study, is accepted to be the ratio of the output force to the input force.

### 3.3 Range of Study

Applying pressure at states  $L_m$  of function  $\delta(\theta, m)$  will increase the angle between links  $OB$  to the maximum value at states  $N_m$ . At states  $L_m$ , HM is in unsteady equilibrium. At states  $N_m$ , HM is in steady equilibrium. This study will investigate the general state of the motion range  $(L_m - N_m)$ . This range exist in all HM family members. Particularly for  $m = 2$  the range is  $(\pi / 2 - 5 \pi / 6)$ , for  $m = 3$  the range is  $(5 \pi / 12 - 2 \pi / 3)$  with parameters  $r = 1.7 m$ ; ;  $p = 3 / 4$ ;

### 3.4 Research Method

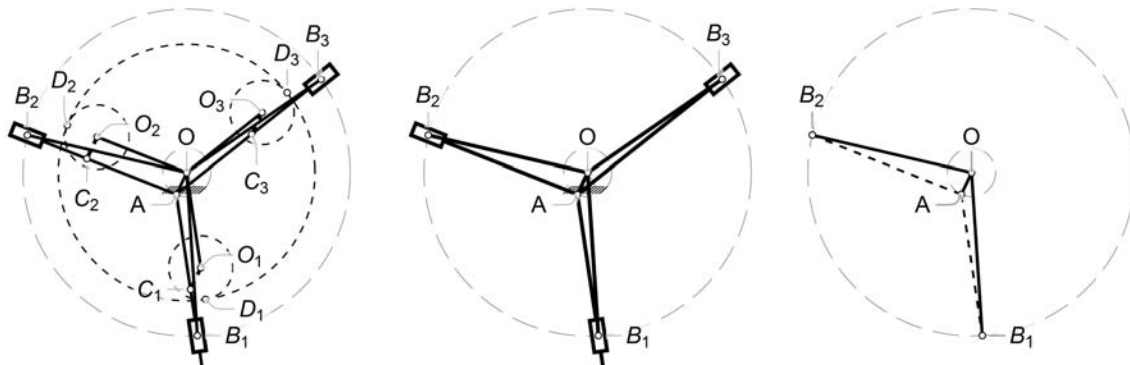
In order to study the HM mechanical advantage it would be most appropriate to use the power method, i.e. how the output force is influenced by an input force from the minimum  $L_m$  to the maximum  $N_m$  of function  $\delta(\theta, m)$ , considering that input power must be equal to output power.

### 3.5 About Parameters

Parameters  $p$  and  $r$  in this study are fixed. At the present time they are considered optimal for engine with angular modul 2 and 3.

### 3.6 Graphic Simplification

The kinematic diagram of HM with angular modulus 3 is in Fig. 11a. The kinematic equivalent simplifies also the graphical representation of the HM by excluding gears. The kinematic equivalent diagram of HM with angular modulus 3 is in Fig. 11b. The graphic simplification used in this study is in Fig. 11c.



a) Kinematic diagram;      b) Kinematic equivalent diagram;      c) Kinematic diagram for this study

Fig. 11 - Kinematic diagrams of HM with  $m=3$ ;  $r=1.7m$ ; ;  $p=3/4$ ;

Fig. 11 is an example with  $m = 3$ . A similar example can be given for every angular modulus. For the purposes of the present study, joints  $B$  and joint  $A$  in Fig. 11c are important.

## 4. Power

### 4.1 Equations

Constraint (8) consists of three energy self-containing joints:  $A$ ,  $(B - A)$  and  $B$  with equal power. Joint  $A$  has only one branch. Joints  $(B - A)$  and  $B$  have  $m$  branches. In this study only the first branch of joint  $B$  will be considered due to the limits outlined in Chapter 3. Joint  $B$  accepts the mechanism input power. Joint  $A$  releases the mechanism output power. The time derivatives of constraint (8) are the velocities of the respective joints in (14). Because  $\dot{\theta} = 1$  according (5) the time derivatives of (14) are equal to the derivatives of local variable  $\theta$  in (16) and (17). The derivatives of local variable  $\theta$  express only geometric parameters and can be used for mechanical advantage calculation.



$$V_p(\theta, m) = \frac{d}{d\theta} \mathbf{A} = m p \begin{bmatrix} -\sin(m\theta) \\ \cos(m\theta) \end{bmatrix} \quad (16)$$

$$V_r(\theta, m) = \frac{d}{d\theta} \mathbf{B} = r \left( 1 - \frac{(m+1)p \cos((m+1)\theta)}{\sqrt{r^2 - p^2 \sin^2(\theta(m+1))}} \right) \begin{bmatrix} -\sin\left(\theta - \sin^{-1}\left(\frac{p \sin((m+1)\theta)}{r}\right)\right) \\ -\cos\left(\theta - \sin^{-1}\left(\frac{p \sin((m+1)\theta)}{r}\right)\right) \end{bmatrix} \quad (17)$$

$$\omega_p(\theta, m) = m \begin{bmatrix} -\sin(m\theta) \\ \cos(m\theta) \end{bmatrix} \quad (18)$$

$$\omega_r(\theta, m) = \left( 1 - \frac{(m+1)p \cos((m+1)\theta)}{\sqrt{r^2 - p^2 \sin^2(\theta(m+1))}} \right) \begin{bmatrix} -\sin\left(\theta - \sin^{-1}\left(\frac{p \sin((m+1)\theta)}{r}\right)\right) \\ -\cos\left(\theta - \sin^{-1}\left(\frac{p \sin((m+1)\theta)}{r}\right)\right) \end{bmatrix} \quad (19)$$

where:  $V_p(\theta, m)$  - velocity of output joint **A**;  $V_r(\theta, m)$  - velocity of input joint **B**;  $\omega_p(\theta, m)$  - angular velocity of output joint **A**;  $\omega_r(\theta, m)$  - angular velocity of input joint **B**;

$$W(\theta, m) = F_{out} V_p(\theta, m) = F_{out} p \omega_p(\theta, m) = F_{in} V_{rm}(\theta, m) = F_{in} r \omega_{rm}(\theta, m) \quad (20)$$

$$MA = \frac{F_{out}}{F_{in}} = \frac{V_{rm}(\theta, m)}{V_p(\theta, m)} = \frac{r \omega_{rm}(\theta, m)}{p \omega_p(\theta, m)} = \frac{V_r(\theta + 2\pi/m, m) - V_r(\theta, m)}{V_p(\theta, m)} = r \frac{\omega_r(\theta + 2\pi/m, m) - \omega_r(\theta, m)}{p \omega_p(\theta, m)} \quad (21)$$

where:  $V_p(\theta, m)$  - velocity of output joint **A**;  $V_r(\theta + 2\pi/m, m)$ ,  $V_r(\theta, m)$  - velocities of input joints **B**;  $\omega_p(\theta, m)$  - angular velocity of output joint **A**;  $\omega_r(\theta + 2\pi/m, m)$ ,  $\omega_r(\theta, m)$  - angular velocities of input joints **B**;  $p$  - length of **A**;  $r$  - length of **B**;  $F_{out}$  - output force;  $F_{in}$  - input force;  $W$  - power;  $MA$  - mechanical advantage

Fig. 12 illustrates forces  $F_{in}$  and  $F_{out}$  on joints **A** and **B**.

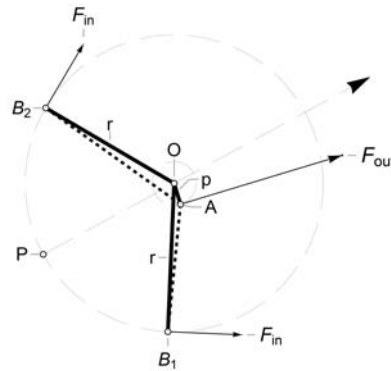


Fig. 12 - Input and output forces on joints **A** and **B**.

Legend: P - origin of forces  $F_{in}$ ; ;  $r$  - length of links  $AB_1$  and  $AB_2$ ;  $p$  - length of link  $OA$ ;  $F_{in}$  - forces on joints **B**;  $F_{out}$  - force on joint **A**;

## 4.1 Power and Velocities

### 4.1.1 HM with Angular Modulus 2

#### 4.1.1.1 Angular velocities

Angular velocities  $\omega(\theta)$  at joints **A** and **B** are in Fig. 13

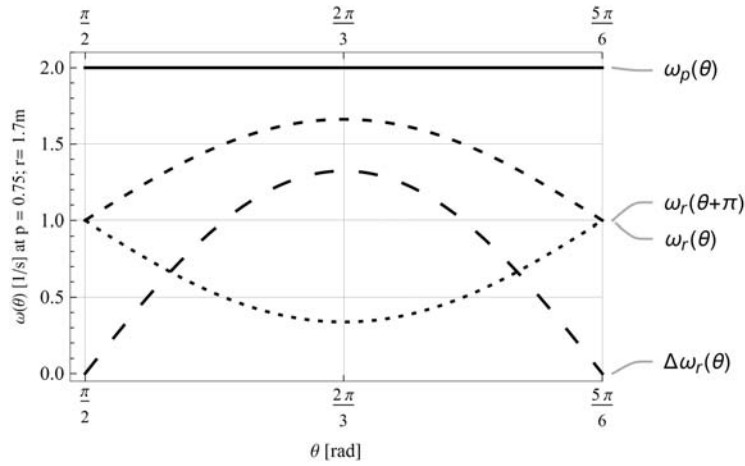


Fig. 13 - Angular velocities at joints *A* and *B* of HM with  $m = 2$

Legend:  $\omega_p(\theta)$  - angular velocity at joint *A* (20);  $\omega_r(\theta)$ ,  $\omega_r(\theta + \pi)$ - angular velocities at joints *B* (21);  $\Delta\omega_r(\theta)$  - difference between angular velocities at joints *B*;  $p$  - crankshaft;  $r$  - invariable link (piston link);  $\theta$ ,  $m$  - HM prototypical parameters;

#### 4.1.1.2 Power

Power  $W$  is presented for joints *B* assuming  $F_{in} = 1$  in Fig 14.

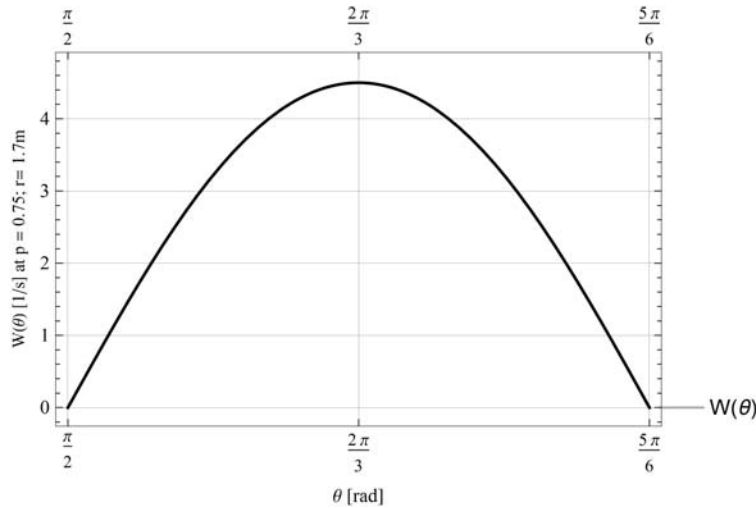


Fig. 14 - Power  $W(\theta)$  at joints *B* of HM with  $m = 2$

Legend:  $p$  - crankshaft;  $r$  - invariable link (piston link);  $\theta$ ,  $m$  - HM prototypical parameters;

### 4.1.2. HM with Angular Modulus 3

#### 4.1.2.1 Angular velocities

Angular velocities  $\omega(\theta)$  at joints *A* and *B* are in Fig. 15

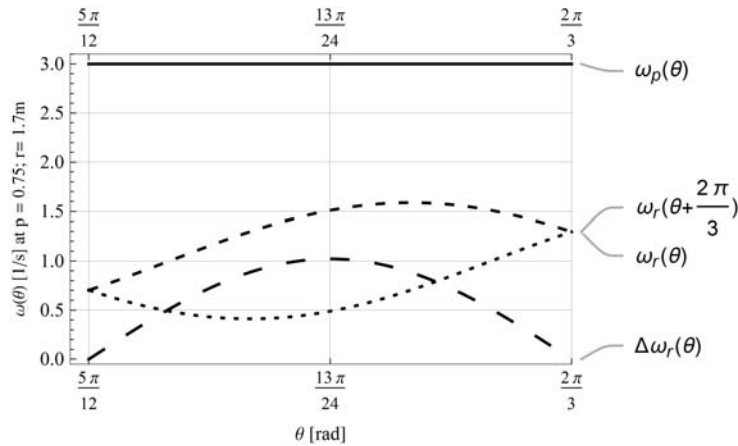


Fig. 15 - Angular velocities at joints **A** and **B** with HM of  $m = 3$

Legend:  $\omega_p(\theta)$  - angular velocity at joint **A** eq.(20);  $\omega_r(\theta)$ ,  $\omega_r(\theta + 2\pi/3)$ - angular velocities at joints **B** eq.(21);  $\Delta\omega_r(\theta)$  - difference between angular velocities at joints **B** ;  $p$  - crankshaft;  $r$  - invariable link (piston link);  $\theta$ ,  $m$  - HM prototypical parameters;

#### 4.1.2.2 Power

Power  $W$  is presented for joints **B** assuming  $F_{in} = 1$  in Fig 16

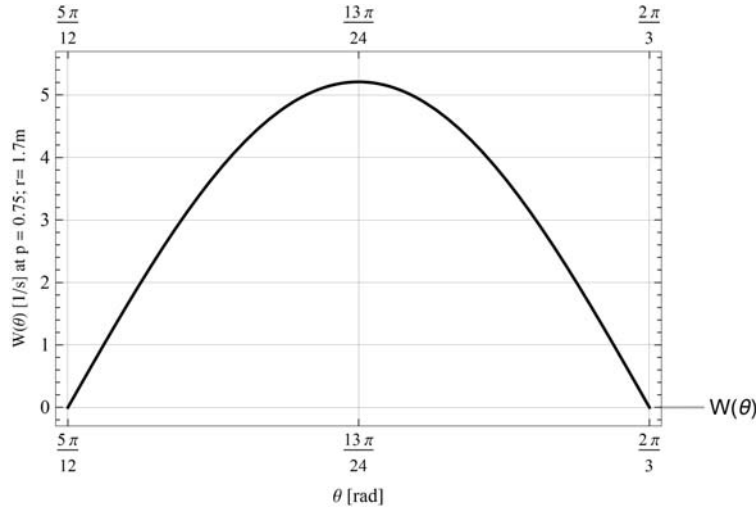


Fig. 16 - Power  $W(\theta)$  at joints **B** of HM with  $m = 3$

Legend:  $p$  - crankshaft;  $r$  - invariable link (piston link);  $\theta$ ,  $m$  - HM prototypical parameters;

## 5. Mechanical Advantage

### 5.1 HM with Angular Modulus 2

Graphics of mechanical advantage for  $m = 2$  according (21) is on fig. 17

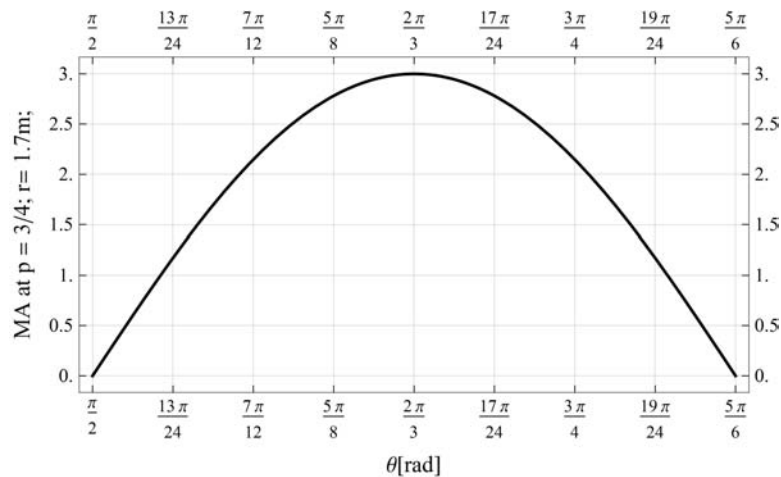


Fig. 17 - HM mechanical advantage at  $m = 2$

Legend: MA - mechanical advantage;  $p$  - crankshaft;  $r$  - invariable link (piston link);  $m$ ,  $\theta$  - HM prototypical parameters;

$$\max MA_2 = 3$$

### 5.2 HM with Angular Modulus 3

Graphics of mechanical advantage for  $m = 3$  according (21) is on fig. 18

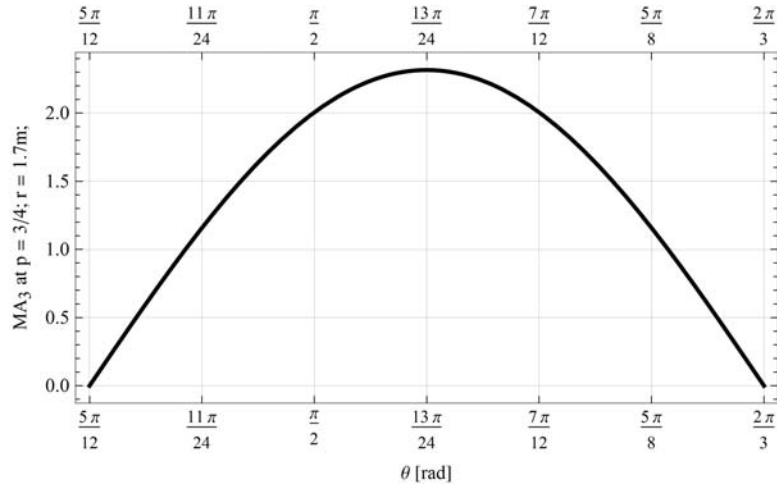


Fig. 18 - HM mechanical advantage at  $m = 3$

Legend: MA - mechanical advantage; p - crankshaft; r - invariable link (piston link); m,  $\theta$  - HM prototypical parameters;  
 $\max MA_3 = 2.31567$

## 6. Validation

Kinematic modeling software was used to prove the validity of the theoretical results. Input forces are applied according to the kinematic diagram in Fig. 14. Instead of output force a motor is attached to the output shaft.

### 6.1 Parameters Setup

There were two “free” parameters to establish: angular velocity of the motor/crankshaft and input forces.

The consideration about the motor/crankshaft angular velocity magnitude is: choosing a magnitude of 1 rad/sec creates m times smaller angular velocity of input joints and the power of the input joints will be equal to the power of output joints where the torque magnitude will be the power magnitude. This consideration reflects the relations in equations (4) and (5). Strictly speaking, a magnitude of 1 rad/sec converts software velocity values to geometric parameters allowing the calculation of the mechanical advantage. This is equivalent to the conversion of (14) to (16) and (17).

The consideration about the input forces is pragmatic: in order to control the output torque the preferable choice was between 1,10 and 100 Newton. 1 Newton was too small, 100 Newton created humungous forces on the screen. An input force of 10 Newton was chosen. Another issue was the scale of the geometric parameters. A scale of (100 : 1) in millimeters turned out to be the most suitable one compared to the graphics and examples in this article.

### 6.2 Dimensions

See Fig. 4 and Fig. 6 for notations. The model dimensions have additional subscript “mo”.

Model of HM with angular modulus 2

$$G_{rmo} = 300 \text{ mm}; g_{rmo1} = g_{rmo2} = 100 \text{ mm}; m_{mo} = 2; p_{mo} = OA = 75 \text{ mm}; r_{mo} = OB_1 = OB_2 = 1.7m_{mo} = 340 \text{ mm};$$

Model of HM with angular modulus 3

$$G_{rmo} = 400 \text{ mm}; g_{rmo1} = g_{rmo2} = g_{rmo3} = 100 \text{ mm}; m_{mo} = 3; p_{mo} = OA = 75 \text{ mm}; r_{mo} = OB_1 = OB_2 = 1.7m_{mo} = 510 \text{ mm};$$

where:  $G_{rmo}$  – radius of model internal gear;  $g_{rmo}$  - radius of model planet gears;  $p_{mo}$  - model crankshaft OA length;  $r_{mo}$  - model invariable links OB length;  $m_{mo}$  - model angular modulus;

### 6.3 Exported Data Sets

12 data sets clusters for each module were exported. The following are the minimum required data sets: Motor torque, Motor angular velocity, Joints **B** velocity and angular velocity.

### 6.4 Graphical Results

A copy of the raw data set of HM models is in Appendix B

### 6.4.1 HM with Angular Modulus 2

#### 6.4.1.1 Power

The co-relation of input and output power is the proof that the model is built and performs correctly. This is shown in Fig. 19

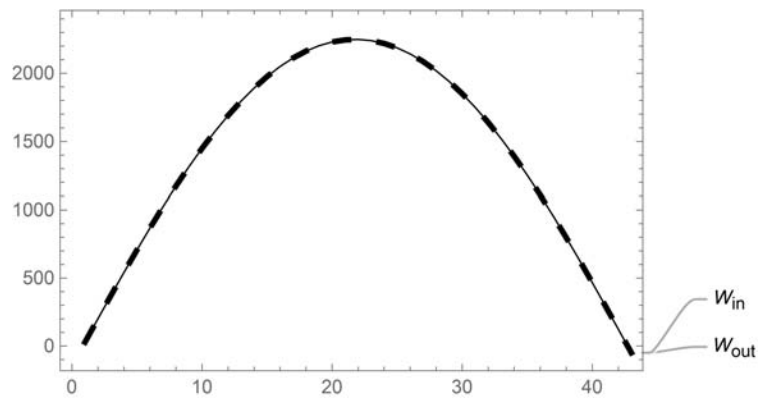


Fig. 19 - Input/Output power of HM model with  $m = 2$

Legend:  $W_{in}$  - input power;  $W_{out}$  - output power;

#### 6.4.1.2 Mechanical advantage

The plot of the mechanical advantage calculated with model data is in Fig. 20

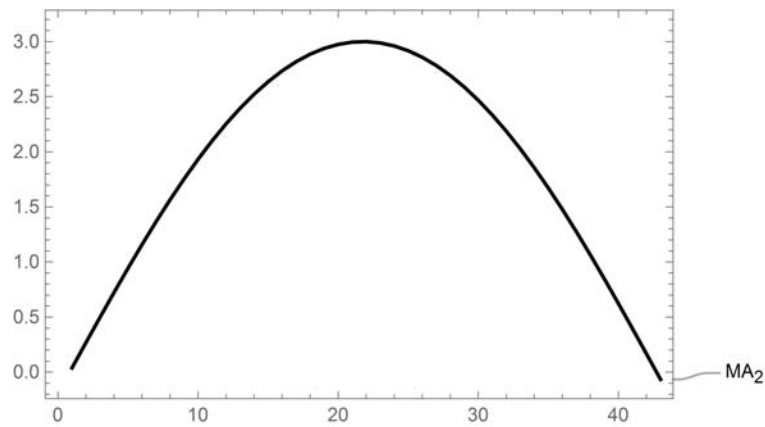


Fig. 20 - Mechanical advantage of HM model with  $m = 2$

Legend:  $MA_2$  - mechanical advantage

$$MA[[22]] = 2.99959$$

### 6.4.2 HM with Angular Modulus 3

#### 6.4.2.1 Power

The HM model of angular modulus 3 is also correct - Fig. 21

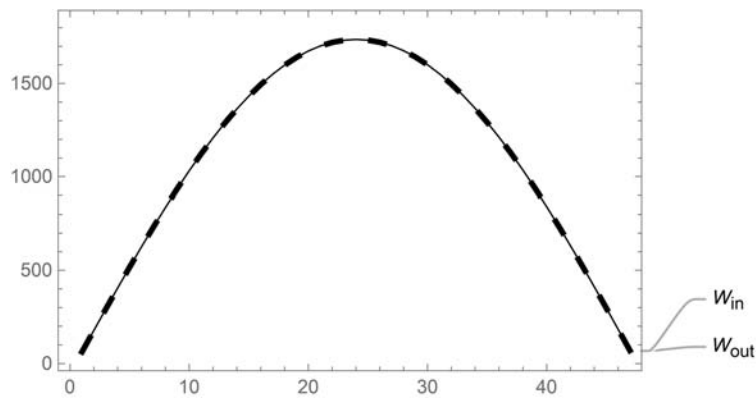


Fig. 21 - Input/Output power of HM model with  $m = 3$

Legend:  $W_{in}$  - input power;  $W_{out}$  - output power;

### 6.4.2.2 Mechanical advantage

The plot of the mechanical advantage calculated with model data is in Fig. 22

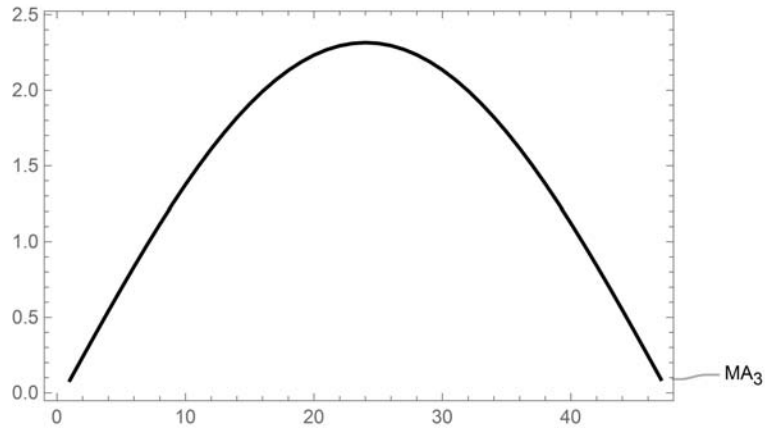


Fig. 22 - Mechanical advantage of HM model with  $m = 3$

Legend:  $MA_3$  - mechanical advantage

$$MA[[24]] = 2.31548$$

## 7. Comparison

### 7.1 Preliminary

The new valveless rotary engine mechanism is the HM described in this paper. Therefore, comparing the mechanical advantage of HM and the inline slider crank mechanism (iSCM) is imperative. The comparison must include the same “index of merit” and parameters used for HM. The inline slider crank mechanism is shown in Fig. 23.

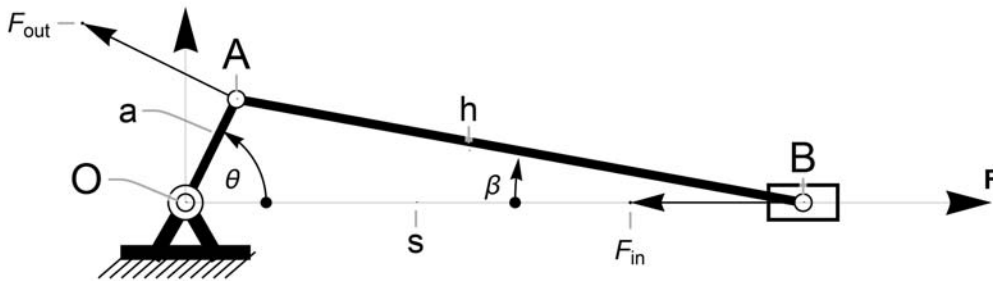


Fig. 23 - The inline slider crank mechanism

Legend:  $a = OA$  - crankshaft;  $h = AB$  - coupler;  $s = OB$  - ground link;  $\theta$  - crankshaft angle;  $\beta$  - coupler angle;

$F_{in}$  - input force;  $F_{out}$  - output force;  $F$  - frame;

### 7.2 Trigonometric Relations

$$\beta = \sin^{-1}\left(\frac{a \sin \theta}{h}\right) \tag{22}$$

$$s = a \cos(\theta) + h \cos(\beta) \tag{23}$$

where:  $h$  - coupler;  $a$  - crankshaft;  $\theta$  - crankshaft angle;  $\beta$  - coupler angle;  $s$  - distance  $OB$ ;

### 7.3 Power Relations

The constraint equation between input and output joints (Fig. 23) has the form [8]

$$C : (\mathbf{B} - \mathbf{A}) \cdot (\mathbf{B} - \mathbf{A}) - h^2 = 0$$

$$\text{where : } \mathbf{A} = a \begin{bmatrix} \cos(\theta) \\ \sin(\theta) \end{bmatrix}; \mathbf{B} = \begin{bmatrix} s \\ 0 \end{bmatrix}; h - \text{coupler}; \quad (24)$$

The derivative of (24) gives relations between the velocities of input and output joints of the mechanism, i.e. the speed ratio

$$\dot{C} = 2 (\mathbf{B} - \mathbf{A}) \cdot (\dot{\mathbf{B}} - \dot{\mathbf{A}}) \partial_t = (s - a \cos(\theta)) \dot{s} + a s \sin(\theta) \dot{\theta} = 0 \quad (25)$$

$$S_r = \frac{\dot{\theta}}{\dot{s}} = - \frac{s - a \cos(\theta)}{a s \sin(\theta)} \quad (26)$$

$$W = F_{in} \dot{s} = F_{out} a \dot{\theta} \quad (27)$$

$$\frac{F_{out}}{F_{in}} = \frac{\dot{s}}{a \dot{\theta}} = - \frac{s \sin(\theta)}{s - a \cos(\theta)} = \frac{\sin(\theta) (a \cos(\theta) + h \cos(\beta))}{h \cos(\beta)} \quad (28)$$

where: a - crankshaft; s - distance OB;  $\dot{\theta}$  - crankshaft angular velocity;  $\dot{s}$  - piston velocity;  $F_{in}$  - input force;  $F_{out}$  - output force;  $S_r$  - speed ratio;  $W$  - power;

## 7.4 Mechanical Advantage

Simplifying (28)

$$MA_{SC} = \sin(\theta) \left( 1 + \frac{a h \cos(\theta) \sqrt{1 - \frac{a^2 \sin^2(\theta)}{h^2}}}{h^2 - a^2 \sin^2(\theta)} \right) \quad (29)$$

where: a - crankshaft (Fig. 23); h - coupler (Fig. 23);  $\theta$  - crankshaft angle (Fig. 23);  $MA_{SC}$  - iSCM mechanical advantage;

Fig. 24 shows MA of iSCM with different parameters a and b with equivalent length to the parameters of HM.

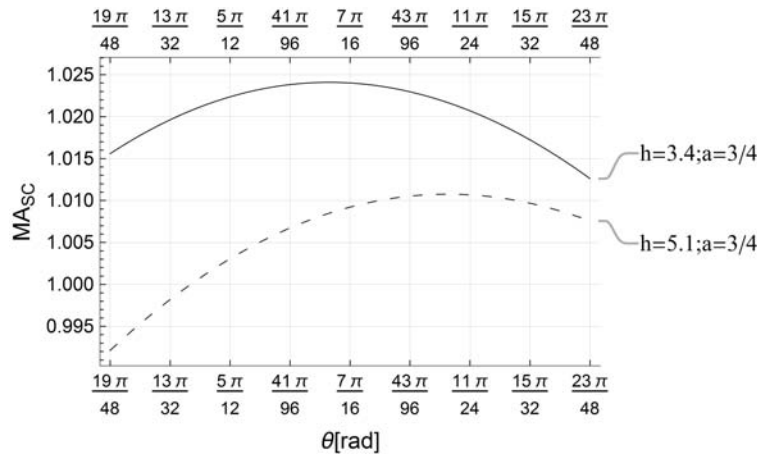


Fig. 24 - iSCM mechanical advantage with different parameters a,h

Legend:  $MA_{SC}$  - mechanical advantage of iSCM; a - crankshaft; h - coupler;  $\theta$  - shaft angle;

The maximum  $MA_{SC}$  value has iSCM with  $h = 3.4$ ;  $b = 3/4$ ; and is below 1.025. The average maximum value of slider crank mechanism mechanical advantage is approximately 1.017 for the parameters equivalent to HM parameters.

## 8. Discussion

This paper is the first attempt to explore the field of the newly created trochoid mechanisms. This is both good and bad news. It is good news because there is no kinematic template to follow, and bad news - for the same reason. Definitely good is the news that research is not necessary for the mechanisms in this field. Definitely bad is the news that while plowing this virgin field the creation of kinematic templates is necessary.

HM has two prototypical parameters -  $\theta$  and  $m$ . Parameter  $m$  identifies each member of the family, and one important feature of a

member - the constant angle between two adjacent invariant links of the rotor. That is why, the name of  $m$  in its birth certificate is: angular modulus.

HM is a mechanism, while the proposed kinematic equivalent is not, according Reuleaux [4]. The kinematic equivalent is a simple closed kinematic chain with 1 DOF (CKC1DOF). CKC1DOF allows derivation of all the kinematic equations like a mechanism. Borrowing the kinematic notations, CKC1DOF can be described as rRPRR, where the new letter “r” stands for the dependent joint. An extra feature of CKC1DOF is the modified Gruebler [5] criterion in eq. (7). Similar CKC1DOFs can be the kinematic equivalents of other aforementioned trochoid mechanisms. CKC1DOF is a new animal in the kinematic zoo.

The application of HM in the real world is revealed in international patent publication WO2020164679 - METHODS AND MACHINES WITH RECIPROCATING AND ROTATING PISTONS WITH POSITIVE DISPLACEMENT from 20.08.2020. The publication describes three trochoid machines - two epitrochoid, and one hypotrochoid which can be an engine. The international patent publication describes the hypotrochoid engine in detail. The mechanism of the hypotrochoid valveless rotary engine in WO2020164679 is presented in Chapter 1 of the present paper. The mechanism of this engine is with angular modulus 3.

The mechanical advantage of the hypotrochoid mechanism is superior compared to the major competitor on the market of internal combustion engines - the slider crank mechanism.

## 9. Conclusion

The loop kinematic equations for a new HM family are derived using a closed kinematic chain as a kinematic equivalent of the mechanism. The derived equations show that the HM mechanical advantage is 3 for angular modulus  $m = 2$ , and the HM mechanical advantage is 2.32 for angular modulus  $m = 3$ . The mechanical advantage equations are validated 99.99% using kinematic modeling software. This mechanical advantage is approximately 2.3 to 3 times higher than that of the inline slider crank mechanism.

## Acknowledgments

I am grateful to my children for their patience and love.

## References

- [1] Mukhopadhyay U., A journey along some well-known curves, 2004, 9(3):33-41, Resonance, DOI:10.1007/BF02834986
- [2] Yates, R. C., Curves and Their Properties, 1974, National Council of Teachers of Mathematics, Library of Congress 74-10222
- [3] Saff E.B., Snieder A.D., Fundamentals of Complex Analysis with Applications..., 2013, Pearson, ISBN 13: 978-1-292-02375-5
- [4] Reuleaux F., The kinematics of machinery, 1876, Macmillan and Co.
- [5] Gruebler M., Getriebelehre, 1917, Springer, ISBN 13: 978-3-662-32126-3
- [6] Hartenberg R.S., Denavit J., Kinematic Synthesis of Linkages, 1964, McGraw-Hill, Library of Congress 64-23251
- [7] Waldron K.J., Kinzel G.L., Kinematics, dynamics, and design of machinery, 2004, Wiley, ISBN 10: 0-471-24417-1
- [8] Michael McCarthy J., Gim Song Soh, Geometric Design of Linkages, 2011, Springer, ISBN 10: 0-939-6047
- [9] Uicker J.J. Jr., Pennock G.R., Shigley J.E., Theory of Machines and Mechanisms, 2016, Oxford, ISBN 13: 978-0-190-26448-2
- [10] Wilson C.E., Sadler P.J., Kinematics and Dynamics of Machinery, 2014, Pearson, ISBN 13: 978-1-292-04005-9
- [11] Myszka, D.H., Machines and mechanisms: applied kinematic analysis, 2012, Pearson, ISBN-13: 978-0-13-215780-3
- [12] Mata A.S. et al, Fundamentals of Machine Theory and Mechanisms, 2016, Springer, ISBN-13: 978-3-279-27968-1

## Appendix A

The relationship of angular velocities in (4) means that the pinion angle of rotation  $m$  times bigger than the carrier angle of rotation. Mathematically speaking the carrier angle of rotation is  $m$ -root of the pinion angle of rotation. In the case of an epicycloid, angle  $\theta$  is an argument of complex number  $z = \cos(\theta) + i \sin(\theta)$ . It follows that,  $m$ -root of  $z$  will be  $z_m = \cos(\theta_m) + i \sin(\theta_m)$  and the argument of  $z_m$  will be  $\theta_m = \theta / m + 2 k \pi / m$ ,  $k = 0, 1, 2, \dots, m-1$ . Theoretically,  $k$  is bigger than  $m - 1$  but all values bigger than  $m - 1$  will cycle over the values equal or less than  $m - 1$ . Consequently, the roots will split the unit circle into  $m$  equal parts, each with an arc length of  $2 \pi / m$ . That is the positive root of  $z$ , where angles  $\theta$  and  $\theta_m$  rotate in the same direction. To explain the rotational invariant of a hypocycloid, a negative root of  $z$  is needed, i.e.  $-z_m = \cos(\theta_m) - i \sin(\theta_m)$ , where  $\theta_m = \theta / m + 2 k \pi / m$ ,  $k = 0, 1, 2, \dots, m-1$ . Here angles  $\theta$  and  $\theta_m$  rotate in the opposite direction. Like in the previous case, the roots will split the unit circle into  $m$  equal parts, each with an arc length of  $2 \pi / m$ .



## Appendix B

### Validation raw data

#### B.1 HM with Angular Modulus 2

##### B.1.1 Output torque

```
Out[226]= {29.1344, 201.867, 373.292, 542.309, 707.847, 868.878, 1024.43, 1173.58,
1315.5, 1449.41, 1574.62, 1690.51, 1796.54, 1892.23, 1977.19, 2051.08, 2113.61,
2164.56, 2203.75, 2231.06, 2246.38, 2249.68, 2240.95, 2220.21, 2187.52,
2143., 2086.8, 2019.12, 1940.21, 1850.37, 1749.97, 1639.44, 1519.3, 1390.11,
1252.52, 1107.27, 955.154, 797.051, 633.9, 466.701, 296.501, 124.387, -48.5338}
```

##### B.1.2 Input angular velocity 1

```
Out[236]= {-0.504285, -0.529685, -0.554892, -0.579745, -0.604087, -0.627766, -0.650639, -0.672573,
-0.693442, -0.713134, -0.731547, -0.74859, -0.764183, -0.778257, -0.790752,
-0.801619, -0.810817, -0.818311, -0.824077, -0.828094, -0.83035, -0.830838,
-0.829555, -0.826507, -0.821702, -0.815158, -0.806895, -0.796943, -0.785339,
-0.772129, -0.757365, -0.741112, -0.723443, -0.704444, -0.68421, -0.662848,
-0.640477, -0.617225, -0.59323, -0.56864, -0.543609, -0.518295, -0.492863}
```

##### B.1.3 Input angular velocity 2

```
Out[240]= {-0.495715, -0.470316, -0.445109, -0.420256, -0.395914, -0.372235, -0.349362, -0.327429,
-0.30656, -0.286868, -0.268455, -0.251412, -0.235819, -0.221745, -0.20925,
-0.198383, -0.189186, -0.181691, -0.175925, -0.171908, -0.169652, -0.169164,
-0.170446, -0.173496, -0.178299, -0.184843, -0.193106, -0.203057, -0.214661,
-0.227872, -0.242635, -0.258886, -0.276557, -0.295556, -0.31579, -0.337152,
-0.359523, -0.382775, -0.40677, -0.43136, -0.456391, -0.481705, -0.507137}
```

#### B.2 HM with Angular Modulus 3

##### B.2.1 Output torque

```
Out[284]= {62.5683, 178.029, 292.699, 406.07, 517.637, 626.906, 733.386, 836.617, 936.133, 1031.49,
1122.27, 1208.06, 1288.48, 1363.18, 1431.83, 1494.11, 1549.68, 1598.42, 1640.06,
1674.42, 1701.35, 1720.71, 1732.43, 1736.46, 1732.78, 1721.4, 1702.38, 1675.8, 1641.77,
1600.45, 1552.03, 1496.4, 1434.44, 1366.11, 1291.71, 1211.56, 1126.02, 1035.49,
940.347, 841.029, 737.975, 631.642, 522.505, 411.047, 297.765, 183.162, 67.7459}
```

##### B.2.2 Input angular velocity 1

```
Out[294]= {0.240684, 0.252481, 0.264657, 0.277154, 0.289916, 0.302882, 0.316007,
0.329205, 0.34242, 0.355593, 0.368661, 0.381563, 0.394239, 0.406631, 0.418673,
0.430335, 0.441476, 0.452137, 0.462288, 0.471864, 0.480796, 0.489048, 0.496616,
0.503455, 0.509538, 0.514844, 0.519361, 0.52305, 0.52591, 0.52793, 0.529104,
0.529426, 0.528822, 0.527443, 0.525219, 0.522157, 0.518268, 0.513568, 0.508072,
0.501803, 0.494784, 0.487043, 0.478611, 0.469522, 0.459813, 0.449526, 0.438704}
```

##### B.2.3 Input angular velocity 2

```
Out[298]= {0.22841, 0.217565, 0.207252, 0.197515, 0.188397, 0.179934, 0.172167,
0.165116, 0.158813, 0.153282, 0.148546, 0.144621, 0.141522, 0.139261, 0.137844,
0.13728, 0.137557, 0.13869, 0.140674, 0.143501, 0.147155, 0.151623, 0.156893,
0.162943, 0.169749, 0.177285, 0.185524, 0.194427, 0.20396, 0.214084, 0.224756,
0.235928, 0.247533, 0.259555, 0.271922, 0.284576, 0.297461, 0.310514, 0.323675,
0.336882, 0.350071, 0.363181, 0.37615, 0.388916, 0.401421, 0.413606, 0.425416}
```